https://doi.org/10.5194/bg-2020-76
Preprint. Discussion started: 30 March 2020

Biogeosciences Discussions
Open Access
EGU

Climate change induced a new intermittent regime of convective ventilation that threatens the Black Sea oxygenation status

Arthur Capet[1], Luc Vandenbulcke[1], and Marilaure Grégoire[1]
[1]MAST, FOCUS, University of Liège, Belgium
Correspondence: A. Capet (acapet@uliege.be)

Abstract. The Black Sea is entirely anoxic, except for a thin (∼100 m) ventilated surface layer. Since 1955, the oxygen content of this upper layer has decreased by 44 %. The reasons hypothesized for this decrease are, first, a period of eutrophication from mid 70's to early 90's and, second, a reduction in the ventilation processes, suspected for the recent years. Here we show that the Black Sea convective ventilation regime has been drastically altered by atmospheric warming during the last decade. Since 2008, the prevailing regime is below the range of variability recorded since 1955, and is characterized by consecutive years during which the renewal of intermediate waters does not occur. Oxygen records from the last decade indicate a clear relationship between cold water formation events and oxygenation status at different pycnal levels, suggesting a leading role of convective ventilation in the oxygen budget of the upper intermediate layers. We thus suggest that this regime shift has a significant impact on the oxygenation structure of the Black Sea and on its biogeochemical balance.

1 Introduction

By reducing water density and increasing vertical stratification, global warming is expected to impede ventilation mechanisms in the world ocean and regional seas with potential consequences for the oxygenation of the subsurface layer (Bopp et al., 2002; Keeling et al., 2010; Breitburg et al., 2018). On a global scale, the reduction of ventilation processes constitutes a larger contribution to marine deoxygenation than the warming-induced reduction of oxygen solubility (Bopp et al., 2013). If the reduction in ventilation mechanisms is often evidenced, it remains challenging to determine whether such changes are the signal of natural variability or rather witness a significant regime change attributed to global warming (Long et al., 2016).

The Black Sea provides a miniature global ocean framework where processes of global interest occur at a scale more amendable for investigation. Its deep basin is permanently stratified and the ventilation of the subsurface layer relies in substantial parts on the convective transport of cold, oxygen-rich water formed each winter in the surface. Between 1955 and 2015, the Black Sea oxygen inventory has declined by 40% (Capet et al., 2016), which echoes the significant deoxygenation trend that affected the world ocean over a similar period (Schmidtko et al., 2017).

https://doi.org/10.5194/bg-2020-76
Preprint. Discussion started: 30 March 2020

Biogeosciences Discussions

The permanent stratification of the Black Sea results from two external inflows (Öszoy and Ünlüata, 1997). The saline Mediterranean inflow enters the Black Sea by the lower part of the Bosporus strait, the sole and narrow opening of the Black Sea towards the global ocean. The terrestrial fresh water inflow, for its greatest part, enters the Black Sea on its northwestern shelf. The contrast in density (salinity) between these two inflows maintains a permanent stratification in the open basin (halocline), that prevents the ventilation of the deep layers. This lack of ventilation induces the permanent anoxic conditions that characterize 90% of the Black Sea waters. Between the oxic and anoxic (euxinic) layers, a suboxic zone, where both dissolved oxygen and hydrogen sulphide are below reliable detection limits, is maintained by biogeochemical processes (Stanev et al., 2018).

Just above the main halocline, the ventilation of the Black Sea subsurface waters (~ 50–$100\mathrm{m}$), is ensured by convective circulation. It proceeds from the sinking of surface waters, made colder and denser by loss of heat towards the atmosphere in wintertime (Ivanov et al., 2000). A similar ventilation process is observed, for instance, in the Mediterranean Gulf of Lion (e.g., MEDOC group et al., 1970; Coppola et al., 2017; Testor et al., 2017). In the Black Sea, however, the dense oxygenated waters never reach the deepest parts, as their sinking is restrained at intermediate depth by the permanent halocline. The accumulation of cold waters at intermediate depth forms the so-called Cold Intermediate Layer (CIL). The process of CIL formation thus provides an annual ventilating mechanism that structures the vertical distribution of oxygen (Gregg and Yakushev, 2005; Capet et al., 2016) and, by extension, that of nutrients (Pakhomova et al., 2014) and living components of the ecosystem (Sakınan and Gücü, 2017).

The semi-enclosed character of the Black Sea, superimposed with the fact that ventilation is limited to the first $\sim$100 m, makes it highly sensitive to variations in external forcings. In particular, the variations of atmospheric conditions (eg. air temperature, wind curl) result in pronounced and relatively fast alterations of the Black Sea physical structure (Oguz et al., 2006; Capet et al., 2012; Kubryakov et al., 2016).

While several studies evidenced a warming trend in the Black Sea surface temperature (Belkin, 2009; von Schuckmann et al., 2018), Miladinova et al. (2017) showed that the Black Sea intermediate waters present an even stronger warming trend. This difference between the surface and subsurface temperature trends can be explained by the fact that the CIL dynamics buffers the atmospheric warming trends and minimize its signature in sea surface temperature (Nardelli et al., 2010).

The inter-annual variability in CIL formation can be explained for its larger part on the basis of winter air temperature anomalies (Oguz and Besiktepe, 1999; Capet et al., 2014), although intensity of the basin-wide cyclonic circulation (Staneva and Stanev, 1997; Capet et al., 2012; Korotaev et al., 2014), fresh water budget (Belokopytov, 2011) and the intensity of short-term meso-scale intrusions also play a role (Gregg and Yakushev, 2005; Ostrovskii and Zatsepin, 2016; Akpinar et al., 2017). An extensive description of the CIL dynamics, detailing the contributions and variability of the mechanisms mentioned above was recently provided by (Miladinova et al., 2018). One aspect is particularly relevant to our study: in winter time, the deepening of the mixed layer and the uplifting of isopycnals in the basin center (as the cyclonic circulation intensifies), expose subsurface waters to atmospheric cooling. If a well-formed CIL was present during the previous year, subsurface waters exposed to atmospheric cooling are already cold, which increases the amount of newly formed CIL waters (Stanev et al., 2003). Due to this positive feed-back and to the accumulation of CIL waters formed during successive years, the inter-annual CIL

https://doi.org/10.5194/bg-2020-76
Preprint. Discussion started: 30 March 2020

dynamics is better described when winter air temperature anomalies are accumulated over 3 to 4 years, rather than considered on a year-to-year basis (Capet et al., 2014).

Given this non-linear context, there are reasons to suspect that global warming, by increasing the average air temperature around which annual fluctuations occur, may induce a persistent shift in the regime of the Black Sea subsurface ventilation. Indeed, Stanev et al. (2019) used Argo float data [2005–2018] to highlight a recent constriction of the CIL layer, following a trends leading to the conditions where the CIL, as a layer colder than the underlying waters, would no longer exist, The authors further indicate implications on the Black Sea thermohaline properties, as this recent weakening of the CIL layer goes along with an increasing trends in surface and subsurface salinity, indicative of diapycnal mixing at the basis of the former CIL layer.

Here, we combine different data sources to analyze the variability in the Black Sea intermediate layer ventilation over the last 65 years and in particular, investigate the existence of a statistically significant shift in the CIL formation regime, in regards to the variability observed over this extended period. The hypothesis of a significant regime shift is tested against the more traditional linear and periodic interpretation of the observed trends (e.g. Belokopytov, 2011), as the consequence for Black Sea ventilation and the future of the Black Sea oxygenation status in particular, are drastically different. Our analysis thus aims to isolate annual convective ventilation as a particular component of the complex Black Sea deoxygenation dynamics (Konovalov and Murray, 2001; Capet et al., 2016) that typically involves intricate biogeochemical and physical processes.

Section 2 details the datasets considered to characterize the Black Sea CIL and oxygenation dynamics and the method of regime shifts analysis. In section 3, we analyse the long-term dynamics of the CIL through the lense of regime shift analysis. In section 4, we use the most detailled datasets to relate CIL formation to changes in the Black Sea oxygenation conditions. Section 5, then concludes with a short discussion on

2 Material and methods

2.1 The CIL cold content

While annual CIL formation rates are difficult to assess directly from observations, the status of the CIL can be quantified locally on the basis of vertical profiles of temperature and salinity. This simple indicator, based on routinely monitored variables, provide a suitable metric to combine various sources of data while summarizing an essential aspect of the thermo-haline conditions. The CIL cold content C is defined as the heat deficit within the CIL, integrated along the vertical:

$$C = -c_p \int_{CIL} \rho(z)[T(z) - T_{CIL}]\, dz, \tag{1}$$

with ρ, the in-situ density, c_p, the heat capacity of sea water and $T_{CIL} = 8.35\ ^\circ\mathrm{C}$, the temperature threshold which together with a density criterion $\rho > 1014.5\ \mathrm{kg\,m^{-3}}$, defines the CIL layer over which the integration is performed (Stanev et al., 2003, 2014; Capet et al., 2014). Although the use of a given temperature threshold to define the occurence of convective mixing is subject to discussion, the existence of a fixed threshold to define the CIL as a distinct watermass, and as a signature of its formation process, is evident given the fixed value of $\sim 9^\circ\mathrm{C}$ that characterize the underlying deep waters (Stanev et al., 2019). The above definition has been chosen for correspondence with past litterature.

https://doi.org/10.5194/bg-2020-76
Preprint. Discussion started: 30 March 2020


Biogeosciences Discussions Open Access EGU

C is expressed in units of $\mathrm{J\,m^{-2}}$ and provides a vertically integrated diagnostic which is more informative than, for instance, the temperature at a fixed depth or the depth of a given iso-thermal surface. Although C is a deficit, we inverted the sign of C in comparison with previous literature (Stanev et al., 2003; Piotukh et al., 2011; Capet et al., 2014) for the convenience of working with a positive quantity. Large C values thus correspond to large heat deficit in the CIL, ie. to low temperature in a well-formed CIL layer, which is characteristic of cold years. A decrease in C corresponds to a weakening of cold water formation (typically for warm years), an increase in the intermediate water temperature and/or a decrease in the vertical extent of the CIL.

C has been estimated for each year over the 1955-2019 period using four data sources summarized in Table 1. These sources include in-situ historical (ship-casts) and modern (Argo) observations, as well as empirical and mechanistic modelling (Fig. 1). Annual and spatial average values for the deep sea (depth > 50 m) were derived from each data set, while considering the artifacts induced by uneven sampling in the context of pronounced seasonal and spatial variability.Each data source has particular assets and drawbacks, and involves specific data processing to reach estimates of annual and spatial C averages as described below. All processed annual time-series are made available in netcdf format on a public repository (see 'Data availability').

Argo profilers: The assets of autonomous Argo profilers are a high temporal resolution and the continuous coverage of recent years, which offers unprecedented means to explore the CIL dynamics at fine spatial and temporal scales (Akpinar et al., 2017; Stanev et al., 2019). The drawbacks are the mingled spatial and temporal variability inherent to Argo data, the incomplete spatial coverage, and the lack of data prior to 2005. These data were collected and made freely available by the Coriolis project and programmes that contribute to it (http://www.coriolis.eu.org). The request criteria used were [Bounding box : 40-47N;27-42E; Period (DD/MM/YYYY) : between '01/01/2005' and '31/12/2019'; Data type(s) : ('Argo profiles','Argo trajectory'); Required Physical parameters : ('Sea temperature','Practical salinity'),Quality : Good.] C values were derived from individual Argo profiles (Fig. 1). All available profiles in a given year were averaged to produce the annual Argo time series C^{Argo}. Although homogeneous seasonal sampling can be assumed, we note that the uneven spatial coverage of Argo profiles might induce a bias in the inferred trends. This potential bias stems from the horizontal gradient in C, that is structured radially from the central (lower C) to the peripheral (higher C) regions of the Black Sea (Stanev et al., 2003; Capet et al., 2014). Argo samplings are more abundant in the peripheral regions, which suggests that C^{Argo} might be slightly biased towards high values.

In-situ ship-cast profiles: The asset of ship-based profiles is their extended temporal coverage. The drawbacks are the difficulty to untangle spatial and temporal variability (as for any non-synoptic data source), the uneven sampling effort and the low data availability posterior to 2000. The C^{Ships} time series was provided by the application of the DIVA detrending methodology on ship-cast profiles extracted from the World Ocean Database (Boyer et al., 2009) in the box 40°–47°30' N, 27°–42°E for the period 1955–2011. DIVA is a sophisticated data interpolation software (Troupin et al., 2012) based on a variational approach. The detrending methodology (Capet et al., 2014) provided inter-annual trends, here representative for the central basin, cleared from the artifacts induced by the combination of uneven sampling and pronounced variability along

https://doi.org/10.5194/bg-2020-76
Preprint. Discussion started: 30 March 2020

Biogeosciences Discussions Open Access EGU

Table 1. Overview of the four data sets used to characterize the CIL inter annual variability. Details are provided for each data source in Sect 2.1

Data Set	Rationale	Assets (+) & Drawbacks (-)	References
Ship casts	In-situ profiles analyzed with the DIVA detrending methodology to disentangle spatial and temporal variability.	+ Large time cover + Direct observation - Uneven spatial and seasonal sampling - Annual gaps	Boyer et al. (2009) Capet et al. (2014)
Atmospheric Predictors	Empirical combination of atmospheric descriptors (winter air temperature anomalies) calibrated to reproduce the above time-series.	+ Full time cover - Not observation - Validity of statistical model not granted outside its range of calibration.	Dee et al. (2011) Capet et al. (2014)
GHER3D	3D hydrodynamic model (GHER). Unconstrained simulation (no data assimilation). 5km resolution. ERA-interim atmospheric forcings.	+ Synopticity + Underlying mechanistic understanding - Not observation	Stanev and Beckers (1999) Vandenbulcke et al. (2010) Capet et al. (2012)
Argo	Drifting autonomous profilers. Average of synchronous profiles.	+ Direct observation + Intra-annual resolution - Uneven spatial sampling - Recent years only	Stanev et al. (2013) Akpinar et al. (2017) Stanev et al. (2019)

the seasonal and spatial dimensions. We redirect the reader to the reference study for further details on data sources, data distribution and methodology.

Atmospheric predictors: The statistical model considered here consists in a linear combination of time-lagged winter air temperature anomalies. This model was obtained by a stepwise selection amongst potential descriptor variables (incl. summer and winter air temperature, winds and fresh water discharge), in order to reproduce the inter-annual variability of C^{Ships} (Capet et al., 2014) and proposed as an alternative to the winter severity index defined earlier (Simonov and Altman, 1991). C^{Atmos} is thus naturally representative of the same quantity, i.e. annually and spatially averaged C. The asset of this approach is the opportunity to fill the gaps between observations in past years, using atmospheric reanalysis of 2m air temperature provided by the European Centre for Medium-Range Weather Forecasts (ECMWF) for the period 1980–2013. Its drawbacks lie in its empirical nature and indirect relationship to observable sea conditions. C^{Atmos} was only extracted for the years covered in the

https://doi.org/10.5194/bg-2020-76
Preprint. Discussion started: 30 March 2020

reference study, considering that the potential non-linearity in the air temperature-C relationship may be exacerbated for the low C values typical of recent years.

3D hydrodynamic model: The Black Sea implementation of the 3D hydrodynamic model GHER has been used in several studies (Grégoire et al., 1998; Stanev and Beckers, 1999; Vandenbulcke et al., 2010; Capet et al., 2012). The present simulation uses the set-up presented in Capet et al. (2012) and has been produced without any form of data assimilation, on the basis of the ERA-Interim set of atmospheric forcing provided by the ECMWF data center (Dee et al., 2011). Aggregated weekly outputs of the GHER3D model are made available on a public repository (see 'Data availability'). $C^{3dModel}$ was derived from synoptic weekly model outputs and averaged for each year and spatially over the deep basin (depth $> 50\mathrm{m}$). The assets of this approach are the synoptic coverage in time and space and the mechanistic nature of the model, that implies a reproducible understanding of the process of CIL formation. The drawback lies in the numerical and conceptual error that might affect unconstrained model outputs.

A composite time series was computed as the average of available source-specific series for each year. Given their indirect nature, the two model time series were given a smaller weight when computing this average (0.5 for the model time series, 1 for the others). The composite time series was then used as a synoptic metric indicating on the inter-annual variability of the convective ventilation of the Black Sea intermediate layers.

The consistency of the different CIL cold content data sources is demonstrated by the high correlations obtained between the annual time series (from 0.91 to 0.98, see detailed comparative statistics in appendix A). Despite the small number of overlapping years between certain series, all correlations are significant ($p < 0.05$). The close correspondence between independent time series, issued respectively from strictly observational and purely mechanistic modeling approaches, provides a high confidence in their accuracy and ensures the robustness of the forthcoming analysis.

More precisely, the standard deviations estimated from the different series are similar ($\sim 100\,\mathrm{MJ\,m^{-2}}$), despite their distinct temporal coverage. The root mean square errors that characterize the disagreement between the different data sources remain below this temporal standard deviation (in all but one case, see appendix A for details). This justifies to merge the different sources in a unique composite time series, enabling a robust long term analysis of the variablity in the Black Sea CIL formation.

2.2 Regime shift analysis and descriptive model selection

The inter annual variability of the Black Sea CIL formation is analyzed in the framework of regime shift analysis (Zeileis et al., 2003). The rationale behind this approach is to identify periods over which the times series depicts statistically distinct regimes, ie. during which annual fluctuations take place around distinct averages. Statistical tools are used to judge the relevance of such segmented description, against the null hypothesis that considers annual fluctuations around a fixed average value for the entire time series. More details are given in appendix B.

The problem when choosing among different models to describe a time series, based on the model's ability to reproduce observations, is that any additional parameter involved in a descriptive model automatically reduces the residual sum of squares (RSS) used to assess its descriptive skill. This is particularly clear in the context of regime shift model, where "considering additional parameters" means segmenting the entire period into more distinct periods with specific averages. To decide until

https://doi.org/10.5194/bg-2020-76
Preprint. Discussion started: 30 March 2020

which point the addition of a new change point (ie. a new distinct period) in the regime shift model remains informative, we considered the Akaike Information Criterion (AIC), that assesses the RSS of each model but gives a penalty for the introduction of additional parameters (Akaike, 1974). The model with the smallest AIC should be favored for interpretation. The same approach was used to compare the regime shifts models to the linear and periodic models.

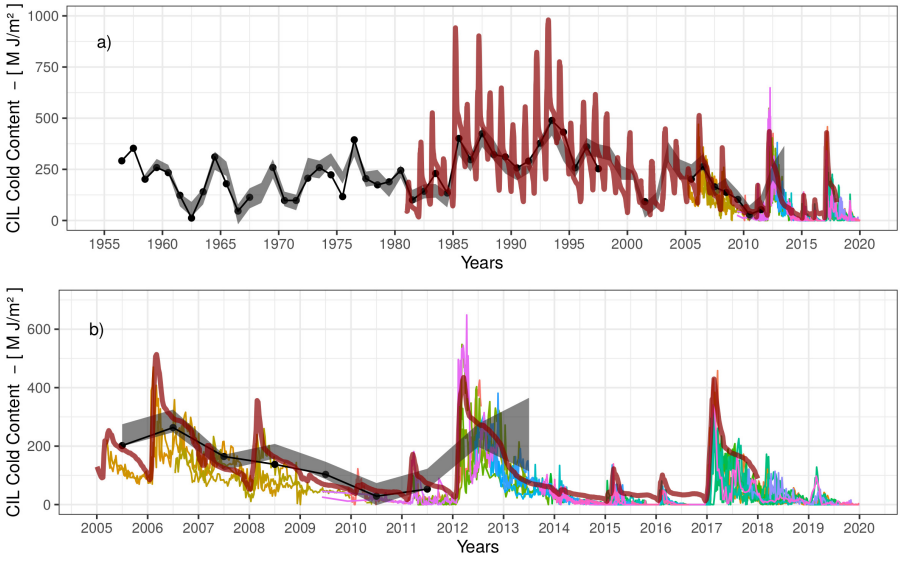

Figure 1. Time series of the Black Sea CIL cold content (C) originated from various data sources (Tab. 1), displayed at original temporal resolution: (black dots) inter-annual trend derived from ship casts; (gray shaded area) statistical model based on atmospheric predictors; (dark red thick line) 3D GHER model; (thin colored lines) Individual Argo floats. a) Complete period of analysis, b) focus on the recent years.

2.3 Oxygen

BGC-Argo oxygen observations were obtained from the Coriolis data center for a period extending from 01/01/2010 to 01/01/2020. Only descending Argo profiles were considered, to minimize discrepancies associated with oxygen sensors response time (Bittig et al., 2014). To minimize the impact of spatial variability, oxygen concentrations were considered using a potential density anomaly (σ) vertical scale and the year 2010 was discarded for lack of observations. While both oxygen concentrations [μM] and oxygen saturation level [%] were considered in our first analyses, the range of thermo-haline variability in the layers considered allow to present only results obtained for one of those aspects and concentration was retained (see Appendix D).

Figure 2 indicates that the use of σ vertical coordinates indeed minimizes the range of spatial variability (see years 2010-2018, when more Argo are operating) and gives sense to the use of monthly medians as an integrated indicator of the basin-wide oxygenation status at different layers. For deeper density layers (Fig. 2c), a larger interquartile range is induced by Argo's

https://doi.org/10.5194/bg-2020-76
Preprint. Discussion started: 30 March 2020

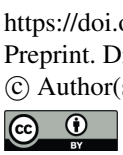

Biogeosciences
Discussions
Open Access
EGU

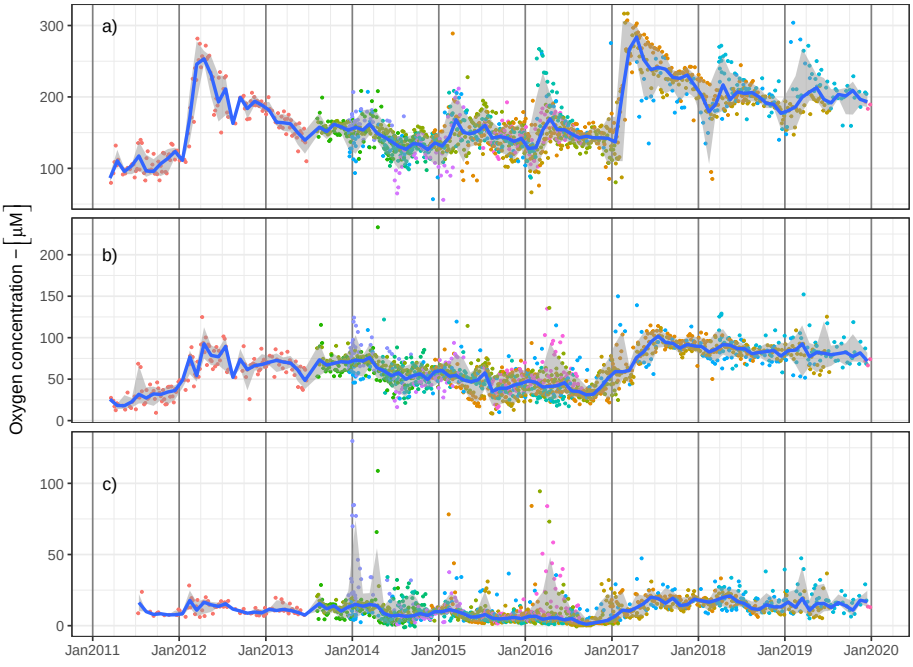

Figure 2. Oxygen concentrations derived from BGC-Argo profiles at σ values of a) 14.5, b) 15.0 and c) 15.5 $\mathrm{kg\,m^{-3}}$. Colored points correspond to different Argo platforms. The blue line represents monthly medians and the shaded area covers monthly interquartile ranges.

profiling in the vicinity of Bosporus influenced area, as plumes of Bosporus ventilation introduce a larger horizontal variability in oxygen concentration.

3 The Black Sea CIL dynamics over 1955–2019

3.1 Descriptive models

The composite time series C_i is depicted on Fig. 3 with calibrated linear and periodic models (with i as a year index).

The poor statistics associated with a linear model, $C_i = l_1.\mathrm{i} + l_2$ (adjusted $R^2 = 0.05$, AIC=794), dismiss the perception of a linear trend extending over the entire period. Using the periodic model, $C_i = p_1 + p_2 \sin(\frac{2\pi}{p_3} i)$, gives a better representation of the cold content inter-annual variability (AIC=763), and provides broad characteristics of C_i : the mean value, $p_1 = 222 \pm 12\ \mathrm{MJ\,m^{-2}}$, the amplitude of inter-annual variability, $p_2 = 114 \pm 16\ \mathrm{MJ\,m^{-2}}$, and the periodicity of pseudo-oscillations, $p_3 = 43.04 \pm 0.02$ years.

However, both the linear and periodic models overestimates C in the recent years, as the composite time series C_i shows a departure from its usual range of variability during the last decade. This is evidenced by ranking the 65 years of C_i on the basis of their cold content. It is remarkable that, among the ten years with the least cold content, eight occurred after 2010.

https://doi.org/10.5194/bg-2020-76
Preprint. Discussion started: 30 March 2020

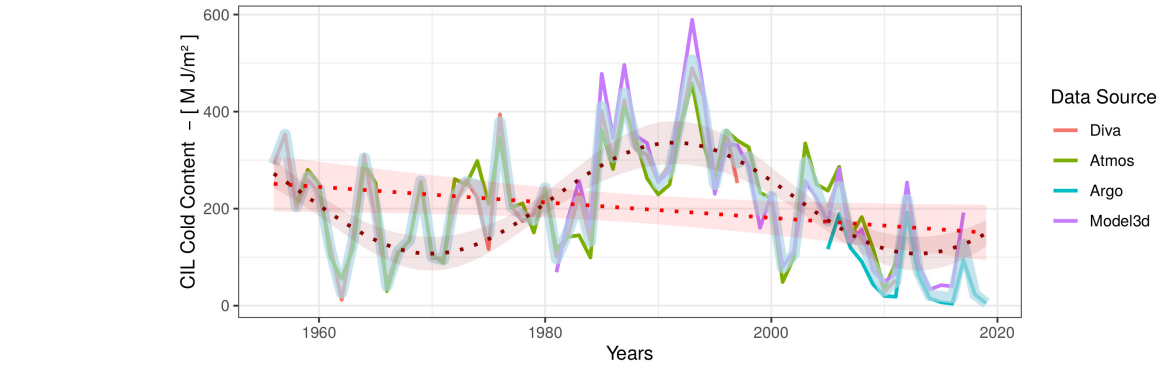

Figure 3. The CIL cold content composite time series (light blue) is obtained as a weighted average of the different data sources. Calibrated linear and periodic models (red dotted lines and area) are considered for discussion.

Figure 4 gives the AIC obtained for regime shifts models considering from 1 to 5 change points (ie. partitioning the entire period into 2 to 6 segments). All of those regime shift descriptions appear as statistically more informative, *sensu* AIC, than a linear or periodic interpretation of the time series (and than a combination of linear and periodic model, AIC=758, not shown). In particular the 4-segments model (ie. 3 change points) should be favored for interpretation.

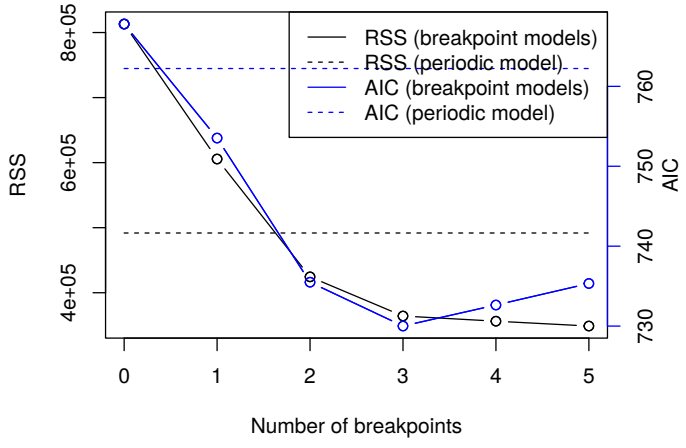

Figure 4. The residual sum of squares (RSS, left scale) of regime shifts models decrease with each additional change points. The Akaike Information Content (AIC, right scale) penalizes additional parameters to support model selection. For comparison, the RSS and AIC obtained with the calibrated periodic model are depicted with dashed lines.

3.2 Regimes shifts in the CIL cold content

The evolution of C_i over 1955-2019 is thus best described by discriminating four periods (P_1–P_4, Fig. 5), objectively identified through regime shift analysis.

https://doi.org/10.5194/bg-2020-76
Preprint. Discussion started: 30 March 2020

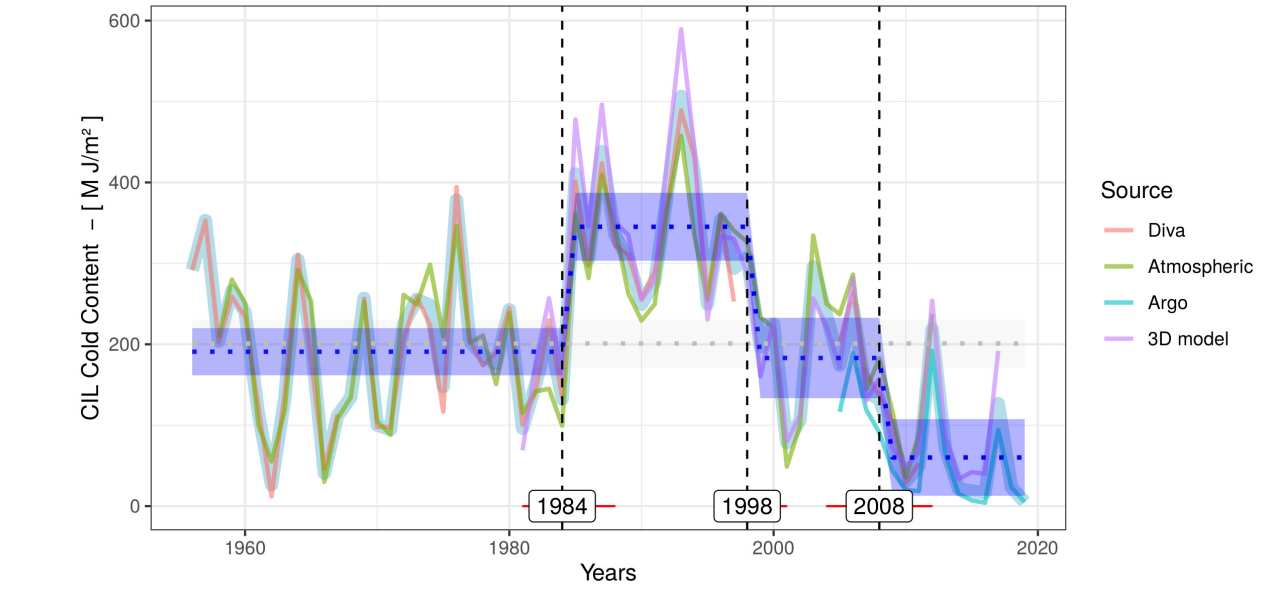

Figure 5. Multi-decadal variability of the Black Sea CIL cold content and distinct periods identified by the regime shift analysis. Confidence intervals on mean C values are indicated by blue shaded area for each period, and by gray shaded area for the null hypothesis (i.e., considering no regime shifts). Confidence intervals on the time limits of each period are indicated with red ranges.

A "routine" regime is identified that is consistent for periods P_1 (1955–1984) and P_3 (1998–2006), which depict averages $\langle C \rangle_{P_1} = 191 \pm 15\,\mathrm{MJ\,m^{-2}}$ and $\langle C \rangle_{P_3} = 183 \pm 29\,\mathrm{MJ\,m^{-2}}$, respectively. This routine regime is also consistent with the average C obtained without considering any change points, $\langle C \rangle = 201 \pm 15\,\mathrm{MJ\,m^{-2}}$ (Fig. 5).

Departing from this routine, a cold period (P_2) is visible from 1984 to 1998, during which C fluctuates around a larger average value, $\langle C \rangle_{P_2} = 345 \pm 26\,\mathrm{MJ\,m^{-2}}$. This cold period has been described in numerous studies (e.g., Ivanov et al., 2000; Oguz et al., 2006), and is attributed to strong and persistent anomalies in atmospheric teleconnection patterns (East Asia/West Russia and North Atlantic oscillations, Kazmin and Zatsepin (2007); Capet et al. (2012)). Noteworthy, similar cold periods were identified earlier in the XXth century (late 1920s–early 1930s and early 1950s, Ivanov et al. (2000)).

From 2008 to 2019, a warmer period (P_4) is identified during which C varies around a lower average $\langle C \rangle_{P_4} = 60 \pm 28\,\mathrm{MJ\,m^{-2}}$. The regime shift analysis thus evidences that a general weakening of the cold water formation and associated ventilation prevails since 10 years in the Black Sea. Warm years and weak cold content were also observed during the years 1961 and 1963, but those were not identified as part of a statistically distinct “warm” regime and should be considered as strong fluctuations within P_1. The regime shift analysis thus indicates that the current restricted ventilation conditions have no precedent in modern history.

https://doi.org/10.5194/bg-2020-76
Preprint. Discussion started: 30 March 2020


Biogeosciences Discussions Open Access EGU

4 CIL formation as a basin-wide ventilation process

The intra-annual resolution provided by the 3D model and Argo time series (Fig. 1) suggests that the CIL renewal, that was taking place systematically each year in precedent regimes, has now become occasional. Here we focus on the latest period, better detailed in our datasets, to characterize the CIL formation as a basin wide ventilation process and its relationship with changes in oxygen concentration at different σ levels.

Basin wide CIL formation and destruction rates were computed from the synoptic 3D model outputs, as differences between weekly C values (Fig. 6). The seasonal sequence depicts CIL formation peaks from late December to March, typically reaching C formation rates of 10, 5 and 1 $\mathrm{MJ\,m^{-2}\,d^{-1}}$ respectively for the period P2, P1-3 and P4. The CIL cold content is then eroded at different rates before, during and at the end the thermocline setting, with a damped erosion rate through the thermocline season between 0 and $\sim$ -1 $\mathrm{MJ\,m^{-2}\,d^{-1}}$. CIL formation processes have been described extensively in the past (e.g. Akpinar et al., 2017; Miladinova et al., 2018), in better details than allowed by the integrated perspective adopted here. This integrated point of view, however, serves to point out the striking quasi absence of CIL formation peak for the years 2001, 2007, 2009, 2010, 2013 and 2014. In fact, among the period of Argo oxygen sampling, only 2012 and 2017 depicts important CIL formation events, while smaller but still perceptible formation rates are observed for 2015 and 2016.

Oxygen concentration in this period varies in concordance with CIL formation until σ layers of about 16.0 (Fig. 7). Large increase in oxygen concentration can be observed from December to March for the years for which CIL formation is significant, which denotes the impact of convective ventilation. While the impact of 2012 and 2017 CIL formation can be seen through the whole oxygenated water column, the smaller CIL formation of 2015 and 2016 only penetrates until $\sim 14.6\,\mathrm{kg\,m^{-3}}$.

Following our attempt to summarize large datasets and to characterize a basin-scale annual oxygenation rate, we computed the difference between the median oxygen concentration in November between successive years. The rationale behind this approach is that CIL formation typically extends from December to March (Fig. 6).

In order to obtain a general indication on the (pycnal) depth of penetration of the convective ventilation associated with CIL formation, we assessed the Pearson correlation coefficient between this annual oxygenation index, and a first order assessment of CIL formation, obtained as the annual difference in the C composite time series. The correlation between oxygenation and CIL formation is high near the surface and decrease regularly as deeper pycnal levels are considered. Those correlations remains significant ($p < 0.1$) until $\sigma = 15.4\mathrm{kg\,m^{-3}}$ (Fig. 8).

5 Discussion

The regime shift paradigm describes an abrupt and significant change in the observable outcome of a non linear-system, as could result from a threshold in this system response to an external forcing. A periodic model, on the other hand, supposes either a linear response to periodically varying external forcing, or an oscillation resulting from internal dynamics. It is our hypothesis, supported by the quantitative consideration presented above, that the first should be favored for interpreting the recent evolution of the Black Sea CIL dynamics. This difference in interpretation is fundamental in what regards the expected consequences on the Black Sea oxygenation status and in particular the threat on Black Sea marine populations, whose ecological adaptation

https://doi.org/10.5194/bg-2020-76
Preprint. Discussion started: 30 March 2020

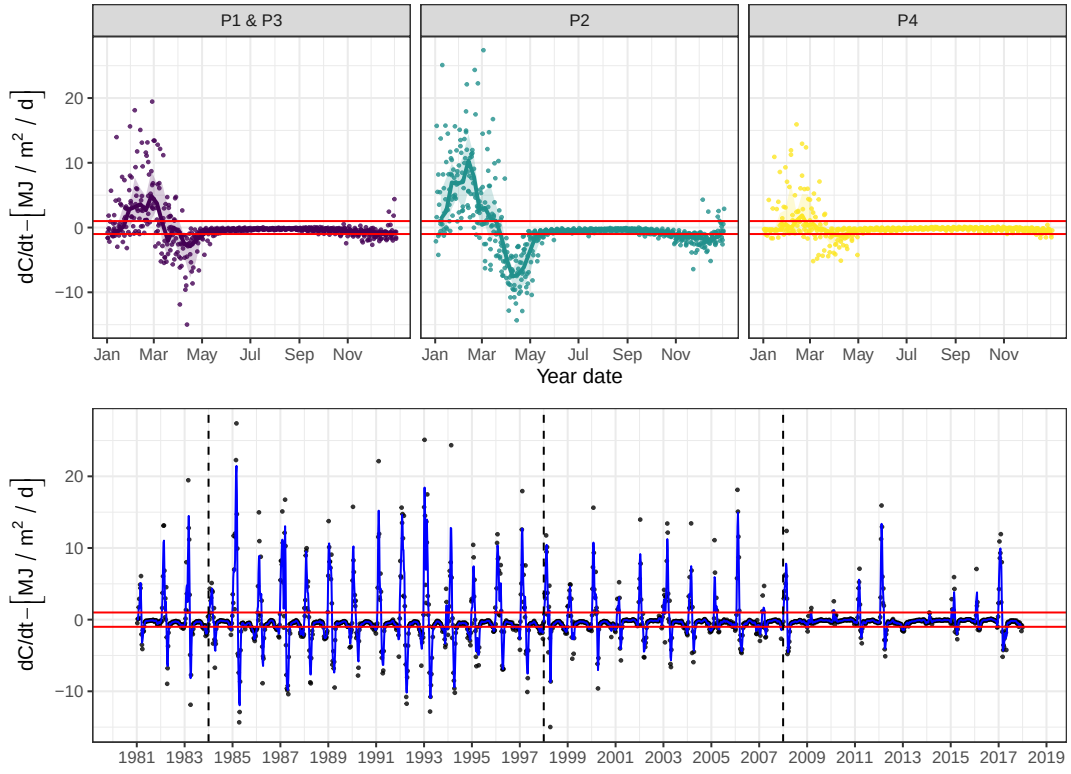

Figure 6. Basin wide CIL cold content formation and destruction rates inferred from the 3D model time-series, weekly averaged values. Upper panels: on a seasonal frame with weekly medians (line) and interquartile range (shaded area), merging years from the periods P1 and P3 (considered together), P2 and P4. Lower panel: on an interannual scale, with 3-weeks running average (blue line). Vertical dotted lines separates the periods evidenced on Fig. 5. The red lines delineate the thresholds of $\pm$ 1 $\mathrm{MJ\,m^{-2}\,d^{-1}}$, corresponding to the lower bound of CIL erosion rate during summers.

(and rate of exploitation) have been build upon a ventilation regime and consequent biogeochemical balance, that may no longer be considered as routine.

It so appears that the intermittency of CIL renewal characterizes the new ventilation regime: the ventilation of the Black Sea intermediate layers does not occur each year anymore but is occasionally absent for one or two consecutive years. As indicated by Stanev et al. (2019), this trends may lead to the disappearance of a characteristic layer of the Black Sea, that constituted a major component of its thermo-haline structure and constrained the exchanges between surface, subsurface and intermediate layers. In particular, the authors highlight surface and subsurface salinity trends that indicate recent occurrences of diapycnal mixing at the lower base of the intermediate layer, where waters are characterized by a strong reduction potential due to the presence of reduced iron and manganese species, ammonium and finally hydrogen sulfide (Pakhomova et al., 2014). Beyond the changes in convective ventilation highlighted above, it thus appears as a lead priority to assess the biogeochemical consequences of this new thermo-haline dynamics of the Black Sea. In particular, the influence of CIL formation on the

https://doi.org/10.5194/bg-2020-76
Preprint. Discussion started: 30 March 2020

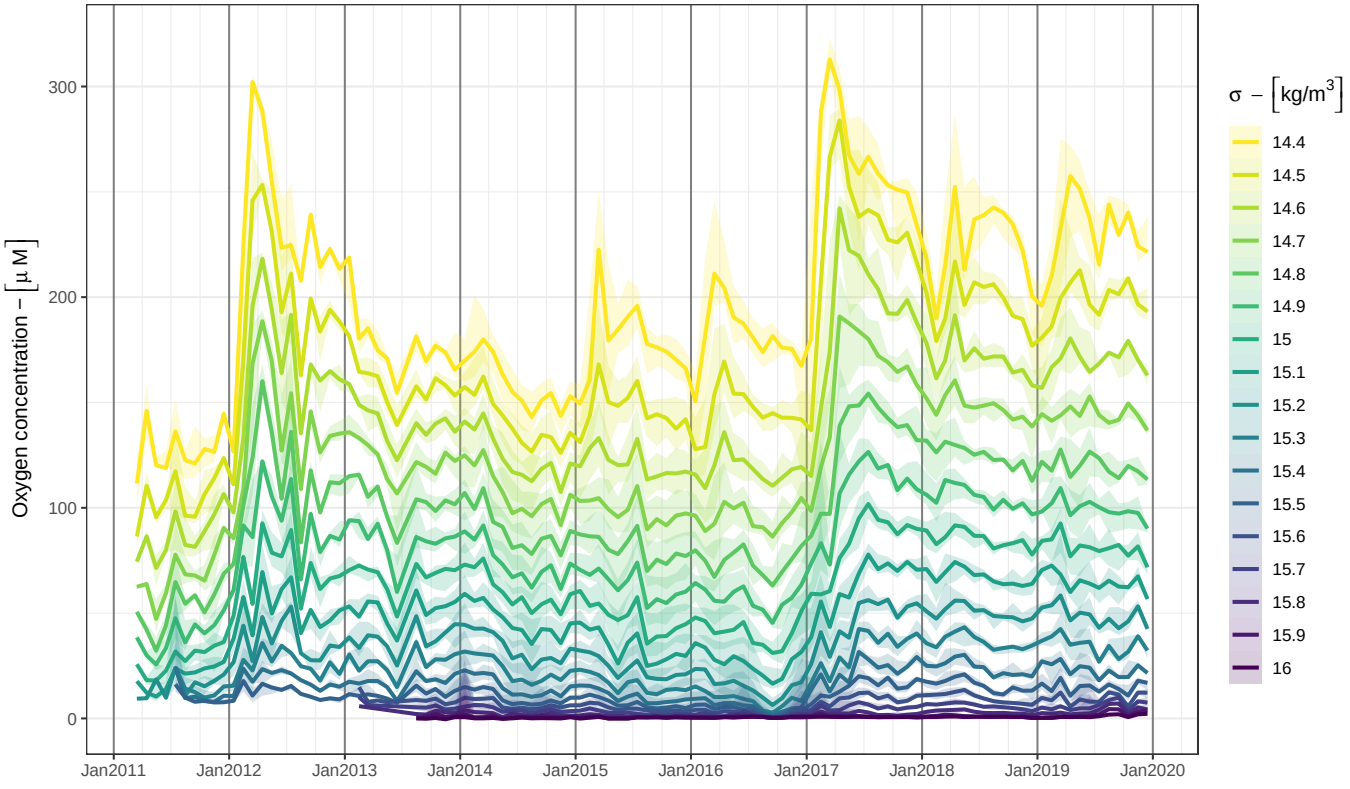

Figure 7. Monthly medians of oxygen concentration at different σ layers. Shaded area indicate the monthly interquartile range (Fig. 2)

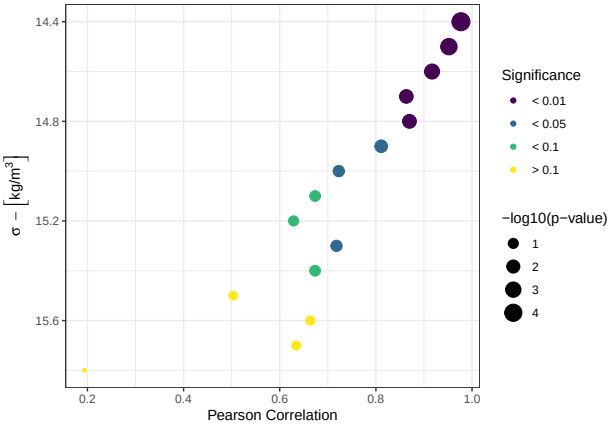

Figure 8. Pearson correlation between basin wide annual oxygenation and CIL formation estimates, for different σ layers. Size of the points relates to the order of magnitude of associated p-values, while colors classify those correlations among classes of significance.

biogeochemical components of the oxygen budget should be addressed in more details, asking for instance how the presence or absence of CIL formation influences on planktonic growth, trophic interactions, and organic matter respiration rates. We

https://doi.org/10.5194/bg-2020-76
Preprint. Discussion started: 30 March 2020

voluntarily adopted here a wide integrative point of view, so as to highlight the large scale relevance of the depicted regime shift on Black Sea oxygenation. However, we still consider that a detailed assessment of all components of the oxygen budget, ie. ventilating processes and biogeochemical production/consumption terms, is required in order to infer the future evolution of the Black Sea oxygenation status (e.g. Grégoire and Lacroix, 2001).

Although, there are clear indications of a long-term warming trend in the Black Sea (Belkin, 2009), it remains a delicate task to strictly dissociate the contributions of global warming from that of regional atmospheric oscillations (Kazmin and Zatsepin, 2007; Capet et al., 2012). One such assessment in the neighboring Mediterranean sea (Macias et al., 2013) concluded that global warming trend and regional oscillation contributed to the recent regional sea surface temperature trend (1985–2009), for respectively 42% and 58%. While corresponding assessment will have to be routinely reevaluated for the Black Sea as time series expand, it may conservatively be considered that global warming had a significant contribution to warming winters in the Black Sea. This contribution is expected to increase in the next decades (Kirtman et al., 2014).

6 Conclusions

We have analyzed the variability of the Black Sea ventilation over the last 65 years and investigated the existence of regime shifts in this dynamics. To this aim, we have produced a composite time series of the CIL cold content (C), that is considered as a proxy for the intensity of the convective ventilation resulting from the formation of dense oxygenated waters. This composite time series is built from four different data products issued from observations and modelling, so as to optimize its temporal extent. The consistency between those products, and in particular the close correspondence between observational and mechanistic predictive time series supports the reliability of the composite series and its adequacy to describe the evolution of the Black Sea subsurface convective ventilation during the last 65 years.

The composite time series was analyzed to detect different regimes, corresponding to periods characterized by significantly distinct averages. Over the last 65 years, we identified 3 main regimes: 1) a routine regime prevailing during 1955–1984 and 1996–2008 that is consistent with the full-period average C, 2) a cold regime (high C, 1984–1996) which as been previously documented (see references in Sect. 3) and 3) a warm regime (low C, 2008–2019) which is characterized by the intermittency of the annual CIL renewal.Statistical considerations indicates that the abrupt shift can not adequately be described by a long term combination of linear and periodic trends.

Clear relationships evidence the role of CIL formation in oxygenating, through convective ventilation, the upper part of the Black Sea intermediate layers (ie. between σ of 14.4 and 15.4 $\mathrm{kg\,m^{-3}}$. Given that cold winter air temperature is the leading driver of CIL formation (Oguz and Besiktepe, 1999; Ivanov et al., 2000; Capet et al., 2014), given that CIL formation constitutes a predominant ventilation mechanism for the Black Sea intermediate layer, and assuming that oxygen conditions constitutes an environmental structuring factor affecting the ecosystem organization, its vigor and its resilience, this shift in the Black Sea ventilation regime may be associated with global warming and is expected to affect its biogeochemical balance and to threaten marine populations adapted to previously prevailing ventilation regimes.

https://doi.org/10.5194/bg-2020-76
Preprint. Discussion started: 30 March 2020

To understand how global warming impacts on the marine deoxygenation dynamics is a worldwide concern. The relatively fast and clear response that stems from the specific Black Sea geomorphology makes it a natural laboratory to study this dependency and related phenomena. Here, we showed that non-linear dynamics and feed-backs in ventilation mechanisms resulted in a significant shift of the average ventilation regime, in response to rising air temperature. Since the temporal extent of low oxygen conditions is critical for ecosystems, we stress the importance to assess the potential for similar ventilation regime shifts in other oxygen deficient basins.

Data availability. The data used are listed in Table 1 Argo data were were collected and made freely available by the Coriolis project[1] and programs that contribute to it. Era-Interim atmospheric conditions were obtained from ECMWF interface[2]. Aggregated weekly outputs of the GHER 3D model, as well as processed annual time series from the different sources are publicly available on a ZENODO repository : https://doi.org/10.5281/zenodo.3691960.

Appendix A: Comparison of the C) time series issued from different data sources

The C time series are noted C_i^m for source m (i is the year index). Each pair of time series (C_i^m, C_i^n) are compared over the years $i \in I^{m,n}$ for which C_i^m and C_i^n are both defined. The following statistics are given for each pair of data sources in Fig. A1 :

- $N^{m,n}$ the number of elements in $I^{m,n}$
- Pearson correlation coefficient :

$$\frac{\sum_{i\in I^{m,n}}(C_i^m-\overline{C^m})(C_i^n-\overline{C^n})}{\sqrt{\sum_{i\in I^{m,n}}(C_i^m-\overline{C^m})^2}\sqrt{\sum_{i\in I^{m,n}}(C_i^n-\overline{C^n})^2}}$$

- The RMS difference between time series :

$$\frac{\sqrt{\sum_{i\in I^{m,n}}(C_i^n-C_i^m)^2}}{N^{m,n}}$$

- The average bias :

$$\frac{\sum_{i\in I^{m,n}}(C_i^n-C_i^m)}{N^{m,n}}$$

[1]http://www.coriolis.eu.org
[2]http://apps.ecmwf.int/datasets/

https://doi.org/10.5194/bg-2020-76
Preprint. Discussion started: 30 March 2020

– The percentage bias :

$$\frac{\sum_{i \in I^{m,n}} (C_i^n - C_i^m)}{\sum_{i \in I^{m,n}} \frac{(C_i^n + C_i^m)}{2}} .100$$

For a better appreciation of variation scales, the temporal standard deviation is also shown for each data source.

The last value of the atmospheric predictor time series (C_{2013}^{Atmos}, Fig. 1. of the main manuscript) was not considered in the composite time series, as it was based on the two, rather than three, predictor values available at the time of publication (hence the larger associated uncertainty). It is remarkable, however, that the published prognostic values for 2012 and 2013, match with independent Argo estimates.

Appendix B: Regime shift analysis

The identification of change points in a time series is the natural first step towards identification of a regime shift (Andersen et al., 2009). The basic change point problem can be expressed as follows: to identify the change point $i = k$ in a sequence x_i of independent random variable with constant variance, such that the expectation of x_i is μ for $i < k$ and $\mu + \Delta\mu_k$ otherwise. Obviously, this problem can be generalized to several change points. The procedure for change point detection is stepwise and has been achieved following the methodology described in the documentation of the R package `strucchange` (Zeileis et al., 2003).

First, the existence of at least one significant change point had to be tested. `strucchange` provides seven statistical tests to compute the p-value at which the null hypothesis of no change points can be rejected. The presence of change points can be tested on the basis of F-Statistic tests or generalized fluctuation tests (Zeileis et al., 2003, and references therein). Table A1 provides the significance level at which the null hypothesis can be rejected for each test implemented in the `strucchange` R package. Among the seven tests considered to assess the presence of at least one significant change point in C_i, 6 rejects the null hypothesis with a significance level $p < 0.05$.

Second, the locations of the N most likely change points were identified. In this study, we considered from one to five change points. The change point locations can be estimated by finding the index values $k_n = [k_1, .., k_N]$ that maximize a likelihood ratio, defined as the ratio of the residual sum of squares for the alternative hypothesis (i.e. change points at k_n with $\Delta\mu_{k_n} \neq 0$) to that of the null hypothesis (i.e. no change point, $\Delta\mu_{k_n} = 0$).

Finally, the choice of a given model (ie. number of change points) had to be considered using the AIC criterion (Sect. 2.2).

Appendix B: Statistics

Formally, the methodology to identify and date structural change is designed for normal random variables, two conditions which can not be granted for environmental time series such as considered here. The following sections detail why 1) the

https://doi.org/10.5194/bg-2020-76
Preprint. Discussion started: 30 March 2020


Biogeosciences Discussions Open Access EGU

Table A1. Tests for the presence of significant structural changes in C_i. p-value indicates the probability that the null hypothesis (i.e. there are no significant change points) should be maintained.

Approach	Test	p-value
F-Statistics	supF test	1.7e-04
	aveF test	5.3e-03
	expF test	1.7e-08
Fluctuations	OLS-based CUSUM test	1.0e-02
	Recursive CUSUM test	3.6e-01
	OLS-based MOSUM test	1.0e-02
	Recursive MOSUM test	1.0e-02

departure of C distribution from a gaussian distribution, 2) the *autocorrelation* in C_i, and 3) the biases between source-specific components of the composite time series C_i, do not affect the conclusions drawn above.

B1 Normality

Skewness in the distribution of C values and its departure from normality is visible at low C values (not shown), as expected for physical reasons: C is a vertically integrated property, naturally bounded by zero. However, the Shapiro-Wilk test that measures the correlation between the quantiles of C_i and those of a normal distribution, indicates no significant departure from normality: $W = 0.975$, $p = 0.23$. For completeness, a Box-Cox transformation ($\lambda = 0.7$) of the original data has been tested which slightly enhances the Shapiro-Wilk test ($W = 0.98$, $p = 0.39$), but brings no sensible alteration in the conclusions of the structural change analysis.

B2 Autocorrelation

Similarly, C_i can not be considered as a random variable. In particular, we introduced in Sect. 1 the CIL preconditioning and partial renewal mechanisms, both physical reasons for which autocorrelation may be expected in C_i. Indeed, correlations between the original and k-lagged time series are, at first glance, significant up to $k = 5$ (Tab. C1, the confidence interval above which autocorrelation can be considered to be significant is given by $1.96/\sqrt{N} = 0.25$). However, it should be considered that the regime shift evidenced in the main manuscript may itself induce apparent autocorrelation statistics. To evidence that this is indeed the case encountered here, the correlation between the original and lagged time series of *the residuals* stemming from the 4–segments model are indicated in Tab. S C1. The fact that no significant autocorrelation persists when change points are considered indicates that the non-randomness of C_i does not jeopardize conclusions drawn from the application of the structural change methodology.

https://doi.org/10.5194/bg-2020-76
Preprint. Discussion started: 30 March 2020

Biogeosciences Discussions Open Access EGU

Table C1. Correlations between (first column) time-lagged replicates of the original C_i and (first column) time-lagged replicates of the residuals of the 4–segment model.

Lag	Original	Residuals
0	1.0	1.0
1	0.57	0.13
2	0.38	-0.22
3	0.32	-0.11
4	0.33	0.03
5	0.26	-0.05

C1 Biases between components of the composite time series

Given that biases exist between different data sources, it might be argued that the composite time series is skewed by the uneven temporal cover of the different sources. For instance if a strongly biased source would solely cover a given period, the composite series would be biased over that period. To ensure that this issue does not affect the presented conclusions, $C_i^{unbiased}$ was constructed as C_i, but removing from each component C_i^m the bias identified identified with the longest C_i^{Ships} time series (which series is used for reference does not impact on structural change conclusions). When $C_i^{unbiased}$ is considered instead of C_i, similar results are obtained in terms of change point models significance and positions of the change points.

Appendix D: Oxygen in situ-data

Oxygen saturation was computed as the percentage of in situ oxygen concentration (converted to μM using in-situ density), with respect to oxygen concentration at saturation, computed considering atmospheric pressure, in-situ temperature and salinity.

Both oxygen concentration and saturation levels were extracted from each Argo profiles at regular σ intervals (14.4 to 16.0 $\mathrm{kg\,m^{-3}}$, by steps of 0.1). Oxygen concentration [μM] is directly relevant as an environmental factor affecting chemical reactions rates. Oxygen saturation level [%] is cleared from the direct temperature effect associated with changes in the solubility of oxygen in seawater, and is arguably more relevant as an environmental factor to represent the impact on living organisms (Vaquer-Sunyer and Duarte, 2011; Roman et al., 2019). However, the range of thermo-haline variability in the subsurface and intermediate layers, on which we focus our analysis of oxygen, is relatively narrow compared to surface waters. Oxygen concentration and saturation level are thus highly correlated for the layer of interest (Fig. D1) and only oxygen concentration is considered in the following .

https://doi.org/10.5194/bg-2020-76
Preprint. Discussion started: 30 March 2020

AC processed the data, set the regime shift methodology, achieved the analyses, issued the visualizations and wrote the initial version of the manuscript. All authors contributed to define the general methodology, to discuss the results and to revise the final mansucript. MG supervised the research.

Competing interests.

No competing interests are identified.

Acknowledgements. This study was funded by the FRS-FNRS FNRS convention BENTHOX (PDR T.1009.15) and directly benefited from the resources made available within the PERSEUS project, funded by the European Commission, grant agreement 287600. LV is funded by the EC Copernicus Marine Environment Service program (contract: BS-MFC). Computational resources have been provided by the supercomputing facilities of the Consortium des Equipements de Calcul Intensif en Federation Wallonie Bruxelles (CECI) funded by the Fond de la Recherche Scientifique de Belgique (FRS-FNRS).

https://doi.org/10.5194/bg-2020-76
Preprint. Discussion started: 30 March 2020

References

Akaike, H.: A new look at the statistical model identification, IEEE transactions on automatic control, 19, 716–723, 1974.

Akpinar, A., Fach, B. A., and Oguz, T.: Observing the subsurface thermal signature of the Black Sea cold intermediate layer with Argo profiling floats, Deep-Sea Res. Pt. I, 124, 140–152, 2017.

Andersen, T., Carstensen, J., Hernandez-Garcia, E., and Duarte, C. M.: Ecological thresholds and regime shifts: approaches to identification, Trends Ecol. Evol., 24, 49–57, 2009.

Belkin, I. M.: Rapid warming of large marine ecosystems, Progr. Oceanogr., 81, 207–213, 2009.

Belokopytov, V.: Interannual variations of the renewal of waters of the cold intermediate layer in the Black Sea for the last decades, Phys. Oceanogr., 20, 347–355, 2011.

Bittig, H. C., Fiedler, B., Scholz, R., Krahmann, G., and Körtzinger, A.: Time response of oxygen optodes on profiling platforms and its dependence on flow speed and temperature, Limnol. Oceanogr., 12, 617–636, https://doi.org/10.4319/lom.2014.12.617, 2014.

Bopp, L., Le Quéré, C., Heimann, M., Manning, A. C., and Monfray, P.: Climate-induced oceanic oxygen fluxes: Implications for the contemporary carbon budget, Global Biogeochem. Cy., 16, 2002.

Bopp, L., Resplandy, L., Orr, J. C., Doney, S. C., Dunne, J. P., Gehlen, M., Halloran, P., Heinze, C., Ilyina, T., Seferian, R., et al.: Multiple stressors of ocean ecosystems in the 21st century: projections with CMIP5 models, Biogeosciences, 10, 6225–6245, 2013.

Boyer, T., Antonov, J., Garcia, H., Johnson, D., Locarnini, R., Mishonov, A., Pitcher, M., Baranova, O., and Smolyar, I.: Chapter 1: Introduction, World ocean database, p. 216, 2009.

Breitburg, D., Levin, L. A., Oschlies, A., Grégoire, M., Chavez, F. P., Conley, D. J., Garçon, V., Gilbert, D., Gutiérrez, D., Isensee, K., et al.: Declining oxygen in the global ocean and coastal waters, Science, 359, eaam7240, 2018.

Capet, A., Barth, A., Beckers, J.-M., and Grégoire, M.: Interannual variability of Black Sea's hydrodynamics and connection to atmospheric patterns, Deep-Sea Res. Pt. II, 77-80, 128–142, https://doi.org/10.1016/j.dsr2.2012.04.010, satellite Oceanography and Climate Change, 2012.

Capet, A., Troupin, C., Carstensen, J., Grégoire, M., and Beckers, J.-M.: Untangling spatial and temporal trends in the variability of the Black Sea Cold Intermediate Layer and mixed Layer Depth using the DIVA detrending procedure, Ocean Dynam., 64, 315–324, 2014.

Capet, A., Stanev, E., Beckers, J.-M., Murray, J., and Grégoire, M.: Decline of the Black Sea oxygen inventory, Biogeosciences, 13, 1287–1297, 2016.

Coppola, L., Prieur, L., Taupier-Letage, I., Estournel, C., Testor, P., Lefèvre, D., Belamari, S., LeReste, S., and Taillandier, V.: Observation of oxygen ventilation into deep waters through targeted deployment of multiple Argo-O2 floats in the north-western Mediterranean Sea in 2013, J. Geophys. Res.-Oceans, 2017.

Dee, D. P., Uppala, S., Simmons, A., Berrisford, P., Poli, P., Kobayashi, S., Andrae, U., Balmaseda, M., Balsamo, G., Bauer, P., et al.: The ERA-Interim reanalysis: Configuration and performance of the data assimilation system, Q. J. Roy. Meteor. Soc., 137, 553–597, 2011.

Gregg, M. and Yakushev, E.: Surface ventilation of the Black Sea's cold intermediate layer in the middle of the western gyre, Geophys. Res. Lett., 32, 2005.

Grégoire, M. and Lacroix, G.: Study of the oxygen budget of the Black Sea waters using a 3D coupled hydrodynamical–biogeochemical model, J. Mar. Syst., 31, 175–202, https://doi.org/10.1016/S0924-7963(01)00052-5, 2001.

Grégoire, M., Beckers, J. M., Nihoul, J. C. J., and Stanev, E.: Reconnaissance of the main Black Sea's ecohydrodynamics by means of a 3D interdisciplinary model, J. Mar. Syst., 16, 85–105, https://doi.org/10.1016/S0924-7963(97)00101-2, 1998.

https://doi.org/10.5194/bg-2020-76
Preprint. Discussion started: 30 March 2020

Ivanov, L., Belokopytov, V., Ozsoy, E., and Samodurov, A.: Ventilation of the Black Sea pycnocline on seasonal and interannual time scales, Mediterr. Mar. Sci., 1, 61–74, 2000.

Kazmin, A. S. and Zatsepin, A. G.: Long-term variability of surface temperature in the Black Sea, and its connection with the large-scale atmospheric forcing, J. Marine Syst., 68, 293–301, 2007.

Keeling, R. F., Körtzinger, A., and Gruber, N.: Ocean deoxygenation in a warming world, Annu. Rev. Mar. Sci, 2, 199–229, https://doi.org/10.1146/annurev.marine.010908.163855, 2010.

Kirtman, B., Power, S. B., Adedoyin, J. A., Boer, G. J., Camilloni, I., Doblas-Reyes, F. J., Fiore, A. M., Kimoto, M., Meehl, G. A., Prather, M., Sarr, A., Schar, C., Sutton, R., van Oldenborgh, G. J., Vecchi, G., and Wang, H. J.: Near-term climate change: projections and predictability, in: Climate change 2013 : the physical science basis : contribution to the Fifth Assessment Report of the Intergovernmental Panel on Climate Change, edited by Stocker, T. F., Qin, D., Plattner, G.-K., Tignor, M. M. B., Allen, S. K., Boschung, J., Nauels, A., Xia, Y., Bex, V., and Midgley, P. M., Cambridge University Press, Cambridge, 2014.

Konovalov, S. K. and Murray, J. W.: Variations in the chemistry of the Black Sea on a time scale of decades (1960–1995), J. Marine Syst., 31, 217–243, 2001.

Korotaev, G., Knysh, V., and Kubryakov, A.: Study of formation process of cold intermediate layer based on reanalysis of Black Sea hydrophysical fields for 1971–1993, Izv. Atmos. Ocean. Phys., 50, 35–48, 2014.

Kubryakov, A. A., Stanichny, S. V., Zatsepin, A. G., and Kremenetskiy, V. V.: Long-term variations of the Black Sea dynamics and their impact on the marine ecosystem, J. Marine Syst., 163, 80–94, 2016.

Long, M. C., Deutsch, C., and Ito, T.: Finding forced trends in oceanic oxygen, Global Biogeochem. Cy., 30, 381–397, 2016.

Macias, D., Garcia-Gorriz, E., and Stips, A.: Understanding the causes of recent warming of mediterranean waters. How much could be attributed to climate change?, PLoS One, 8, e81 591, 2013.

MEDOC group et al.: Observation of formation of deep water in the Mediterranean Sea, 1969, Nature, 227, 1037, 1970.

Miladinova, S., Stips, A., Garcia-Gorriz, E., and Macias Moy, D.: Black Sea thermohaline properties: Long-term trends and variations, J. Geophys. Res.-Oceans, 2017.

Miladinova, S., Stips, A., Garcia-Gorriz, E., and Moy, D. M.: Formation and changes of the Black Sea cold intermediate layer, Progr. Oceanogr., 167, 11–23, 2018.

Nardelli, B. B., Colella, S., Santoleri, R., Guarracino, M., and Kholod, A.: A re-analysis of Black Sea surface temperature, J. Marine Syst., 79, 50–64, 2010.

Oguz, T. and Besiktepe, S.: Observations on the Rim Current structure, CIW formation and transport in the western Black Sea, Deep-Sea Res. Pt I, 46, 1733–1753, 1999.

Oguz, T., Dippner, J. W., and Kaymaz, Z.: Climatic regulation of the Black Sea hydro-meteorological and ecological properties at interannual-to-decadal time scales, J. Marine Syst., 60, 235–254, https://doi.org/10.1016/j.jmarsys.2005.11.011, 2006.

Ostrovskii, A. G. and Zatsepin, A. G.: Intense ventilation of the Black Sea pycnocline due to vertical turbulent exchange in the Rim Current area, Deep Sea Res. Part I, 116, 1–13, 2016.

Öszoy, E. and Ünlüata, U.: Oceanography of the Black Sea: a review of some recent results., Earth-Sci. Rev., 42, 231–272, 1997.

Pakhomova, S., Vinogradova, E., Yakushev, E., Zatsepin, A., Shtereva, G., Chasovnikov, V., and Podymov, O.: Interannual variability of the Black Sea proper oxygen and nutrients regime: the role of climatic and anthropogenic forcing, Estuar. Coast. Shelf S., 140, 134–145, 2014.

https://doi.org/10.5194/bg-2020-76
Preprint. Discussion started: 30 March 2020

Piotukh, V., Zatsepin, A., Kazmin, A., and Yakubenko, V.: Impact of the Winter Cooling on the Variability of the Thermohaline Characteristics of the Active Layer in the Black Sea, Oceanology, 51, 221, 2011.

Roman, M. R., Brandt, S. B., Houde, E. D., and Pierson, J. J.: Interactive Effects of Hypoxia and Temperature on Coastal Pelagic Zooplankton and Fish, Frontiers in Marine Science, 6, 139, https://doi.org/10.3389/fmars.2019.00139, 2019.

Sakınan, S. and Gücü, A. C.: Spatial distribution of the Black Sea copepod, Calanus euxinus, estimated using multi-frequency acoustic backscatter, ICES J. Mar. Sci., 74, 832–846, 2017.

Schmidtko, S., Stramma, L., and Visbeck, M.: Decline in global oceanic oxygen content during the past five decades, Nature, 542, 335, 2017.

Simonov, A. and Altman, E.: Hydrometeorology and Hydrochemistry of the USSR Seas, The Black Sea, 4, 430, 1991.

Stanev, E. and Beckers, J.-M.: Numerical simulations of seasonal and interannual variability of the Black Sea thermohaline circulation, J. Marine Syst., 22, 241–267, 1999.

Stanev, E., Bowman, M., Peneva, E., and Staneva, J.: Control of Black Sea intermediate water mass formation by dynamics and topography: Comparison of numerical simulations, surveys and satellite data, J. Mar. Res., 61, 59–99, https://doi.org/10.1357/002224003321586417, 2003.

Stanev, E., He, Y., Grayek, S., and Boetius, A.: Oxygen dynamics in the Black Sea as seen by Argo profiling floats, Geophys. Res. Lett., 40, 3085–3090, 2013.

Stanev, E. V., He, Y., Staneva, J., and Yakushev, E.: Mixing in the Black Sea detected from the temporal and spatial variability of oxygen and sulfide–Argo float observations and numerical modelling, Biogeosciences, 11, 5707–5732, 2014.

Stanev, E. V., Poulain, P.-M., Grayek, S., Johnson, K. S., Claustre, H., and Murray, J. W.: Understanding the Dynamics of the Oxic-Anoxic Interface in the Black Sea, Geophys. Res. Lett., 45, 864–871, 2018.

Stanev, E. V., Peneva, E., and Chtirkova, B.: Climate Change and Regional Ocean Water Mass Disappearance: Case of the Black Sea, J. Geophys. Res. C: Oceans, 124, 140, https://doi.org/10.1029/2019JC015076, 2019.

Staneva, J. and Stanev, E.: Cold intermediate water formation in the Black Sea. Analysis on numerical model simulations, in: Sensitivity to Change: Black Sea, Baltic Sea and North Sea, pp. 375–393, Springer, 1997.

Testor, P., Bosse, A., Houpert, L., Margirier, F., Mortier, L., Legoff, H., Dausse, D., Labaste, M., Karstensen, J., Hayes, D., et al.: Multiscale Observations of Deep Convection in the Northwestern Mediterranean Sea During Winter 2012-2013 Using Multiple Platforms, J. Geophys. Res.-Oceans, 2017.

Troupin, C., Barth, A., Sirjacobs, D., Ouberdous, M., Brankart, J.-M., Brasseur, P., Rixen, M., Alvera-Azcárate, A., Belounis, M., Capet, A., et al.: Generation of analysis and consistent error fields using the Data Interpolating Variational Analysis (DIVA), Ocean Model., 52, 90–101, 2012.

Vandenbulcke, L., Capet, A., Beckers, J.-M., Grégoire, M., and Besiktepe, S.: Onboard implementation of the GHER model for the Black Sea, with SST and CTD data assimilation, J. Oper. Oceanogr., 3, 47–54, 2010.

Vaquer-Sunyer, R. and Duarte, C. M.: Temperature effects on oxygen thresholds for hypoxia in marine benthic organisms, Glob. Chang. Biol., 17, 1788–1797, 2011.

von Schuckmann, K., Traon, P.-Y. L., Aaboe, S., Fanjul, E. A., Autret, E., Axell, L., Aznar, R., Benincasa, M., Bentamy, A., Boberg, F., Bourdallé-Badie, R., Nardelli, B. B., Brando, V. E., Bricaud, C., Breivik, L.-A., Brewin, R. J., Capet, A., Ceschin, A., Ciliberti, S., Cossarini, G., de Alfonso, M., de Pascual Collar, A., de Kloe, J., Deshayes, J., Desportes, C., Drévillon, M., Drillet, Y., Droghei, R., Dubois, C., Embury, O., Etienne, H., Fratianni, C., Lafuente, J. G., Sotillo, M. G., Garric, G., Gasparin, F., Gerin, R., Good, S., Gourrion, J., Grégoire, M., Greiner, E., Guinehut, S., Gutknecht, E., Hernandez, F., Hernandez, O., Høyer, J., Jackson, L., Jandt, S., Josey, S.,

https://doi.org/10.5194/bg-2020-76
Preprint. Discussion started: 30 March 2020

505 Juza, M., Kennedy, J., Kokkini, Z., Korres, G., Kõuts, M., Lagemaa, P., Lavergne, T., Cann, B. L., Legeais, J.-F., Lemieux-Dudon, B., Levier, B., Lien, V., Maljutenko, I., Manzano, F., Marcos, M., Marinova, V., Masina, S., Mauri, E., Mayer, M., Melet, A., Mélin, F., Meyssignac, B., Monier, M., Müller, M., Mulet, S., Naranjo, C., Notarstefano, G., Paulmier, A., Gomez, B. P., Gonzalez, I. P., Peneva, E., Perruche, C., Peterson, K. A., Pinardi, N., Pisano, A., Pardo, S., Poulain, P.-M., Raj, R. P., Raudsepp, U., Ravdas, M., Reid, R., Rio, M.-H., Salon, S., Samuelsen, A., Sammartino, M., Sammartino, S., Sandø, A. B., Santoleri, R., Sathyendranath, S., She, J., Simoncelli, S.,
510 Solidoro, C., Stoffelen, A., Storto, A., Szerkely, T., Tamm, S., Tietsche, S., Tinker, J., Tintore, J., Trindade, A., van Zanten, D., Verhoef, A., Vandenbulcke, L., Verbrugge, N., Viktorsson, L., Wakelin, S. L., Zacharioudaki, A., and Zuo, H.: Copernicus Marine Service Ocean State Report, J. Oper. Oceanogr., 11, S1–S142, https://doi.org/10.1080/1755876X.2018.1489208, 2018.

Zeileis, A., Kleiber, C., Krämer, W., and Hornik, K.: Testing and dating of structural changes in practice, Comput. Stat. Data An., 44, 109–123, 2003.

https://doi.org/10.5194/bg-2020-76
Preprint. Discussion started: 30 March 2020

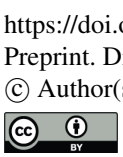

Biogeosciences
Discussions
Open Access
EGU

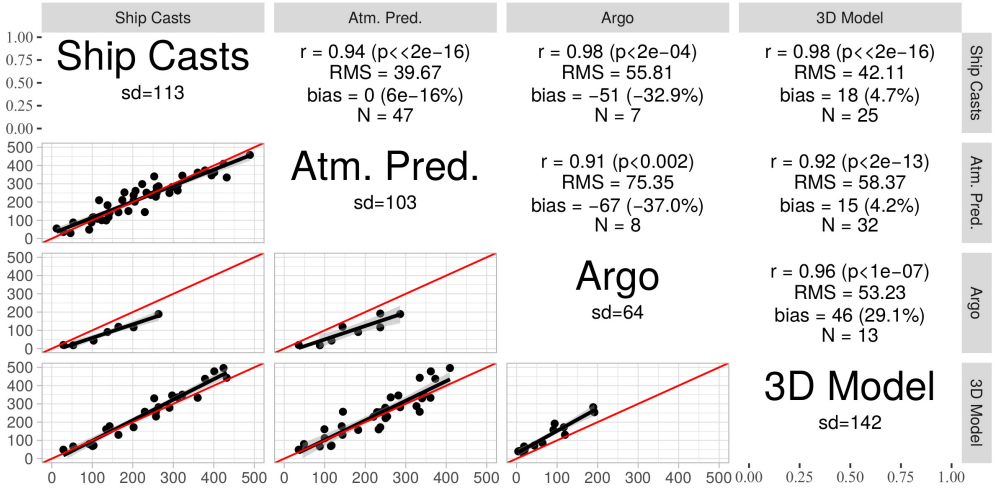

Figure A1. Statistics of comparison between the different data sources.

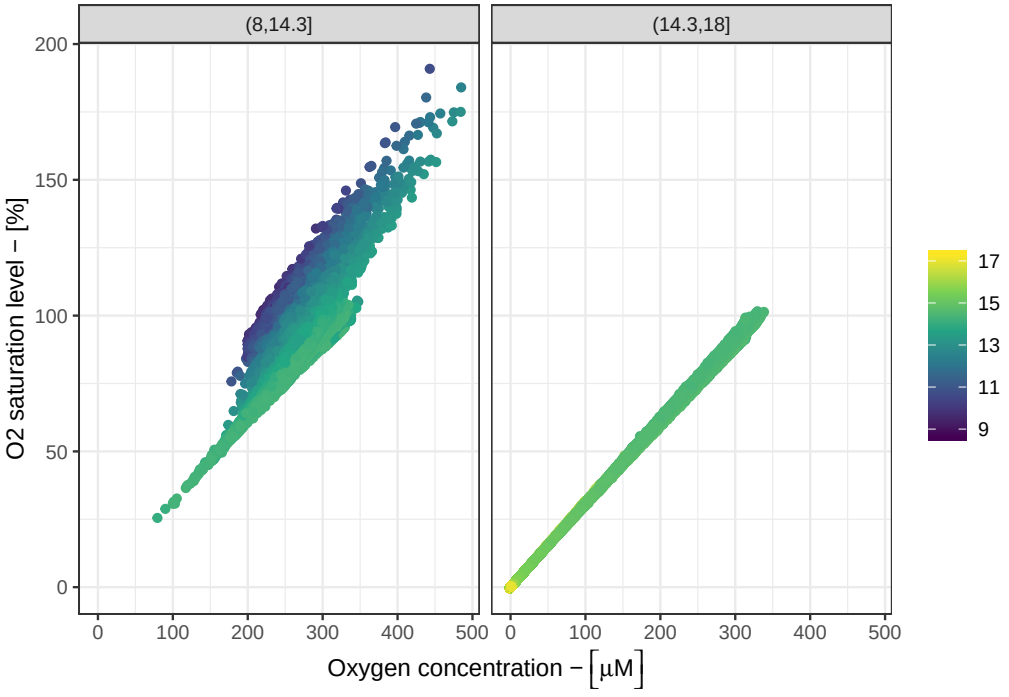

Figure D1.

Oxygen concentration [μM] and oxygen saturation level [%] derived from Argo samplings above (left) and below (right) the isopycnal $\sigma = 14.3 \mathrm{kg\,m^{-3}}$. The color scale gives the potential desnity anomaly associated with each sampling (σ - $\mathrm{kg\,m^{-3}}$).